

## Article

# Physicochemical Characteristics and Hydrolytic Degradation of Polylactic Acid Dermal Fillers: A Comparative Study

Nikita G. Sedush <sup>1,\*</sup>, Kirill T. Kalinin <sup>1</sup>, Pavel N. Azarkevich <sup>1</sup> and Antonina A. Gorskaya <sup>2</sup>

<sup>1</sup> Enikolopov Institute of Synthetic Polymeric Materials, Russian Academy of Sciences, Moscow 117393, Russia; k.kalinin@ispm.ru (K.T.K.); n.azarkevich@ispm.ru (P.N.A.)

<sup>2</sup> Neroly Ltd., Nizhny Novgorod 603155, Russia; neroly@neroly.com

\* Correspondence: nsedush@gmail.com

**Abstract:** Dermal fillers have gained significant attention in the field of aesthetic medicine due to their ability to restore volume and correct facial wrinkles. Even though such formulations have similar compositions, they can have different microstructure and molecular characteristics, which in turn affect the biodegradation profile. This study presents the results of an investigation of the physicochemical characteristics of four dermal fillers from different manufacturers (Sculptra<sup>®</sup>, Gana V<sup>®</sup>, AestheFill<sup>®</sup>, and Repart PLA<sup>®</sup>). The molecular and supramolecular characteristics of polylactic acid (L/D isomer ratio, molecular weight, degree of crystallinity), the morphology and size of PLA microparticles were determined. Hydrolytic degradation studies in phosphate buffer revealed differences in the rate of molecular weight reduction in the polymer. The obtained data may be important for the analysis and interpretation of the results of biological studies and clinical outcomes of the PLA dermal fillers.

**Keywords:** biodegradable polymers; dermal filler; polylactide; microparticles



**Citation:** Sedush, N.G.; Kalinin, K.T.; Azarkevich, P.N.; Gorskaya, A.A. Physicochemical Characteristics and Hydrolytic Degradation of Polylactic Acid Dermal Fillers: A Comparative Study. *Cosmetics* **2023**, *10*, 110. <https://doi.org/10.3390/cosmetics10040110>

Academic Editor: Christophe Hano

Received: 26 June 2023

Revised: 18 July 2023

Accepted: 24 July 2023

Published: 1 August 2023



**Copyright:** © 2023 by the authors. Licensee MDPI, Basel, Switzerland. This article is an open access article distributed under the terms and conditions of the Creative Commons Attribution (CC BY) license (<https://creativecommons.org/licenses/by/4.0/>).

## 1. Introduction

Dermal fillers have found extensive application in the field of cosmetic dermatology for the correction of facial folds and wrinkles, enhancement of facial skin quality, and addressing other medical and aesthetic concerns. These preparations have a rich history spanning over a century [1]. However, it is in the last two decades that dermal fillers have gained remarkable popularity, thanks to the successful development of biocompatible materials that offer a prolonged efficacy with minimal risks of complications. Fillers can be categorized into temporary, permanent, and semi-permanent types based on their biodegradability. Also, they can be classified according to their primary components, which encompass collagen, hyaluronic acid, polylactic acid (PLA), poly( $\epsilon$ -caprolactone), calcium hydroxyapatite, polymethylmethacrylate, polyacrylamide, and autologous fat cells [2]. Recently, the biocompatible and biodegradable polylactic acid [3,4] has drawn increasing attention among cosmetologists, leading to a growing interest in biodegradable fillers based on this polymer. The main mechanism of action of PLA-based fillers lies in their ability to stimulate the production of new collagen through a moderate tissue response.

Fillers based on polylactic acid (PLA) typically comprise a mixture of PLA microparticles and auxiliary components, such as sodium carboxymethylcellulose and mannitol. Despite the similar composition of these formulations, notable variations are often observed in their practical applications, encompassing aspects ranging from the ease of injection to the occurrence of complications. Previous investigations have indicated that the effectiveness and safety of these fillers are closely related to the physicochemical characteristics of the PLA microparticles present within them [5–7]. PLA degradation proceeds through the scission of the ester linkages in the main chain of the polymer, which is induced by hydrolysis due to the sorption of water in microparticles. In the human body, the soluble

degradation products (lactic acid and its oligomers) are metabolized by the cells. The rate of degradation has been found to be dependent on a range of factors, such as the stereochemical composition of the polymer (*L*-to-*D*-isomer ratio), its molecular weight and crystallinity, size, and morphology of the microparticles, pH, enzyme activity, and others. The composition of the polymer and its molecular weight are among the key parameters. The degradation profile of the filler determines the rate of lactic acid formation, which can affect the activity of fibroblasts in the synthesis of collagen. Therefore, understanding the differences in the biological effects of PLA-based fillers may lie in analyzing their physicochemical characteristics and comparing them with the results of *in vivo* experiments and clinical outcomes reported in the literature. While the literature contains information on the *in vitro*, *in vivo*, and clinical studies of some commercial products [8–11], there is a significant lack of reports devoted to the analysis of their physicochemical characteristics. Therefore, the aim of this study is to analyze the key characteristics and hydrolytic degradation of PLA microparticles in four commercial products: Sculptra<sup>®</sup>, Gana V<sup>®</sup>, AestheFill<sup>®</sup>, and Repart<sup>®</sup> PLA.

## 2. Materials and Methods

### 2.1. Sample Preparation

The following polylactic acid-based fillers were studied: Sculptra<sup>®</sup> (Q-Med AB, Uppsala, Sweden), Gana V<sup>®</sup> (Gana R&D, Seongnam, Republic of Korea), AestheFill<sup>®</sup> (REGEN Biotech Inc., Seoul, Republic of Korea), and Repart PLA<sup>®</sup> (Ingal, Moscow, Russia). The composition and key parameters of the formulations claimed by the manufacturers in the manual are presented in Table 1.

**Table 1.** Characteristics of the studied fillers claimed by manufacturers.

Filler	Composition			Degradation Period, Months
	Microparticles	Na-CMC	Mannitol	
AestheFill <sup>®</sup>	154 mg poly( <i>D,L</i> -lactic acid)	46	-	24
Gana V <sup>®</sup>	210 mg poly( <i>L</i> -lactic acid)	132	177	27.6
Repart PLA <sup>®</sup>	154 mg poly( <i>D,L</i> -lactic acid)	46	167.2	24
Sculptra <sup>®</sup>	150 mg poly( <i>L</i> -lactic acid)	90	127.5	24

As indicated in Table 1, the investigated formulations are mixtures of polymeric microparticles and auxiliary components, namely sodium carboxymethylcellulose (Na-CMC) and mannitol. To separate the microparticles from the auxiliary components, the following procedure was performed. Firstly, a sample of the filler (100 mg) was suspended in 2 mL of distilled water and vigorously shaken by vortex until a homogeneous suspension was achieved. Next, the suspension was subjected to centrifugation at 5000 rpm for 5 min to precipitate the microparticles. The supernatant containing water-soluble components (Na-CMC and mannitol) was carefully decanted, and an equal volume of distilled water was added. This process was repeated twice more to ensure the complete elimination of water-soluble components. During the centrifugation of AestheFill and Gana V fillers, along with the precipitate, a floating fraction was formed on the surface due to the porosity of the microparticles. This fraction was also subjected to analysis. Finally, the washed microparticles were flash-frozen in liquid nitrogen and freeze-dried to obtain dry powders for further analysis.

### 2.2. Hydrolytic Degradation Studies

The PLA microspheres (120 mg) isolated from formulations were suspended in 10 mL of phosphate-buffered saline (PBS) with pH = 7.4 and incubated at 37 ± 0.3 °C in a thermostat incubator for a total period of 9 months. The AestheFill microparticles did not form a homogeneous suspension in PBS; therefore, the degradation study of this sample was conducted in distilled water. Samples were collected at 1, 4, 6, and 9 months after the

start of the experiment. To determine the molecular weight and investigate the morphology of the microspheres, the samples were frozen in liquid nitrogen and freeze-dried.

### 2.3. Nuclear Magnetic Resonance

To determine the chemical composition, the samples were dissolved in deuterated chloroform, and the resulting solutions were analyzed using  $^1\text{H}$  nuclear magnetic resonance (NMR) spectroscopy on a Varian-Agilent VNMRs 700 spectrometer.

### 2.4. Gel Permeation Chromatography

The molecular weight characteristics of the polymers were investigated using gel permeation chromatography on a Knauer chromatographic system (Berlin, Germany) equipped with a refractive index detector. The samples were dissolved in tetrahydrofuran (5 mg/mL). The experiments were conducted at a temperature of 40 °C and with an eluent flow rate (tetrahydrofuran) of 1 mL/min. The Agilent PLgel Mixed-C column was calibrated using polystyrene standards.

### 2.5. Scanning Electron Microscopy

The morphology and size of the microspheres were investigated using a Phenom XL scanning electron microscope (Thermo Fisher Scientific, Waltham, MA, USA) equipped with backscattered and secondary electron detectors. The operating pressure was set at 0.1 Pa, and the accelerating voltage was 5 kV. To construct size distribution histograms using the ImageJ software, the size of at least 700 particles was determined. In the case of irregularly shaped particles, the size was determined based on the maximum distance between their points. The size  $D_{av}$  is reported as mean size  $\pm$  standard deviation.

### 2.6. Differential Scanning Calorimetry

Thermal properties and the degree of crystallinity of poly(*L*-lactic acid) were studied using differential scanning calorimetry in dynamic mode on a Perkin-Elmer DSC 7 instrument. The investigations were conducted in a temperature range from  $-20$  to  $200$  °C with a heating rate of  $10$  °C/min.

## 3. Results and Discussion

### 3.1. Molecular Structure and Crystallinity

Poly(lactic acid) (PLA) is a biocompatible and biodegradable polymer, wherein the monomeric unit is lactic acid. This molecule exists in two stereoisomeric forms: *L*-lactic acid and *D*-lactic acid. The polymers composed exclusively of *L*-lactic acid units are referred to as poly(*L*-lactic acid) (PLLA), while those composed of *D*-lactic acid units are known as poly(*D*-lactic acid) (PDLA). In case of an equal ratio of *L*-lactic acid and *D*-lactic acid, the polymer is called poly(*D,L*-lactic acid) (PDLLA). The ratio of *L*- and *D*-units in PLA is a vital characteristic as it governs the physicochemical properties and degradation profile [12]. Due to stereoregular structure, PLLA and PDLA exhibit crystallization ability, whereas PDLLA is entirely amorphous. By manipulating the *L*-to-*D*-lactic acid ratio in PLA, the biodegradation rate of the polymers can be controlled within a broad range, spanning from several months to years. It is worth noting that the kinetics of biodegradation is influenced by various other parameters, including molecular weight, the degree of crystallinity, shape, size, porosity, and more [4]. Moreover, environmental conditions within the organism, such as pH levels and the presence of enzymes, also significantly affect this process.

**Composition.** The composition of the polymer microspheres was determined using  $^1\text{H}$  nuclear magnetic resonance (NMR) spectroscopy; the spectra are presented in Figure 1. The observed *a* and *b* signals correspond to the CH groups (chemical shift 5.15–5.25 ppm) and  $\text{CH}_3$  groups (1.55–1.6 ppm) of polylactic acid, respectively. Upon closer examination of the CH group region, it can be observed that the signals for the Sculptra and Gana V samples exhibit quartets, which is indicative of poly(*L*-lactic acid). In contrast, the Report

PLA and AestheFill samples show a splitting of this signal (the appearance of additional multiplets in the 5.20–5.24 ppm range), which is characteristic of poly(*D,L*-lactic acid).

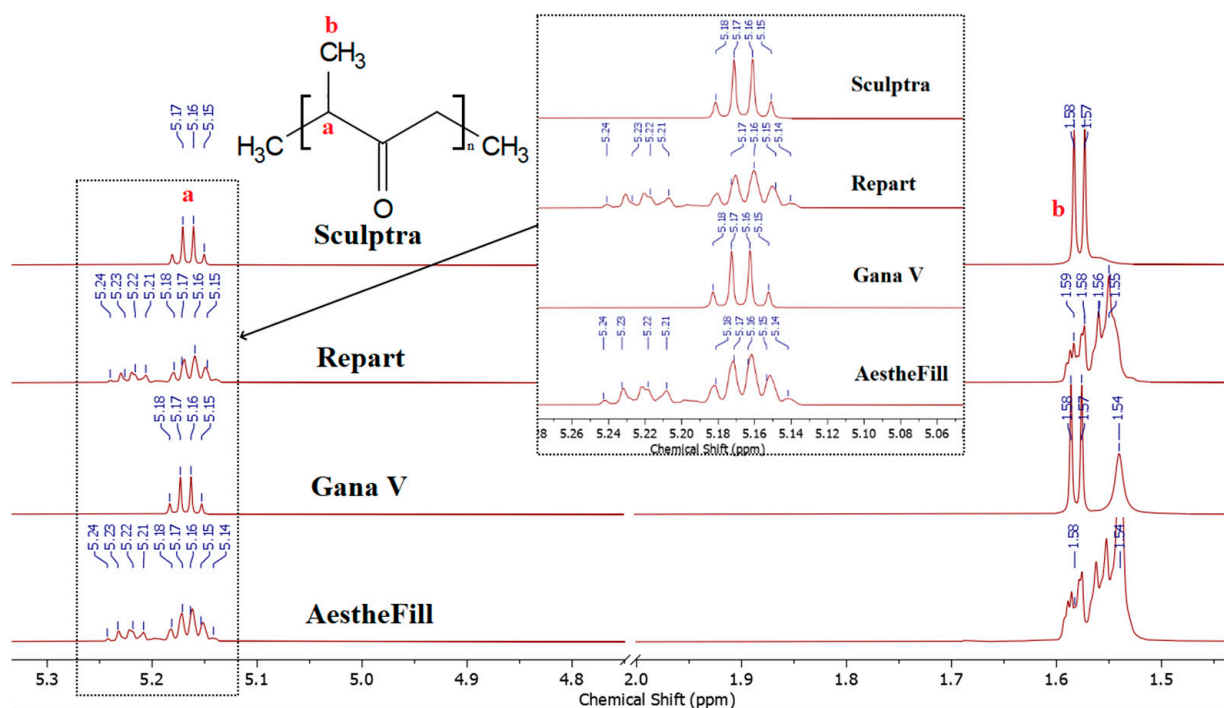


**Figure 1.**  $^1\text{H-NMR}$  spectra of the microspheres ( $\text{CDCl}_3$ ).

Therefore, the results of the NMR spectroscopy confirm that the stereochemical composition of the microspheres corresponds to the one claimed by the manufacturers. The microspheres in Sculptra and Gana V are made of poly(*L*-lactic acid), while Report PLA and AestheFill consist of poly(*D,L*-lactic acid).

**Crystallinity.** It is known that, unlike amorphous poly(*D,L*-lactic acid), poly(*L*-lactic acid) can crystallize. The presence of a crystalline phase in the polymer significantly influences the material's properties, including its degradation rate, as water penetration into polymer crystallites is hindered. Therefore, to determine the degree of crystallinity, the Sculptra and Gana V samples were additionally studied by differential scanning calorimetry (DSC). The DSC curves for the first heating cycle (Figure 2) exhibit endothermic melting peaks in the range of 120–180 °C for both samples, corresponding to the melting of poly(*L*-lactic acid) crystallites. Two or even three melting peaks are observed, indicating the presence of crystallites with varying degrees of imperfection. The total melting enthalpy for the Sculptra and Gana V samples was found to be 60 and 67 J/g, corresponding to a crystallinity degree of 64% and 72%, respectively. One can expect the slower degradation for these microparticles in comparison with fully amorphous poly(*D,L*-lactic acid) analogs since water penetration into a crystalline phase of material is hindered. On the curves of the second heating, transitions corresponding to the polymer glass transition temperature are clearly visible. It was observed at 57 °C for Sculptra and 50 °C for Gana V. Additionally, on the curves of the second heating, exothermic crystallization peaks are observed in the range of 100–130 °C, followed by melting peaks. Such a pattern is characteristic of poly(*L*-lactic acid), which is capable of crystallization due to the stereoregularity of the polymer chain.



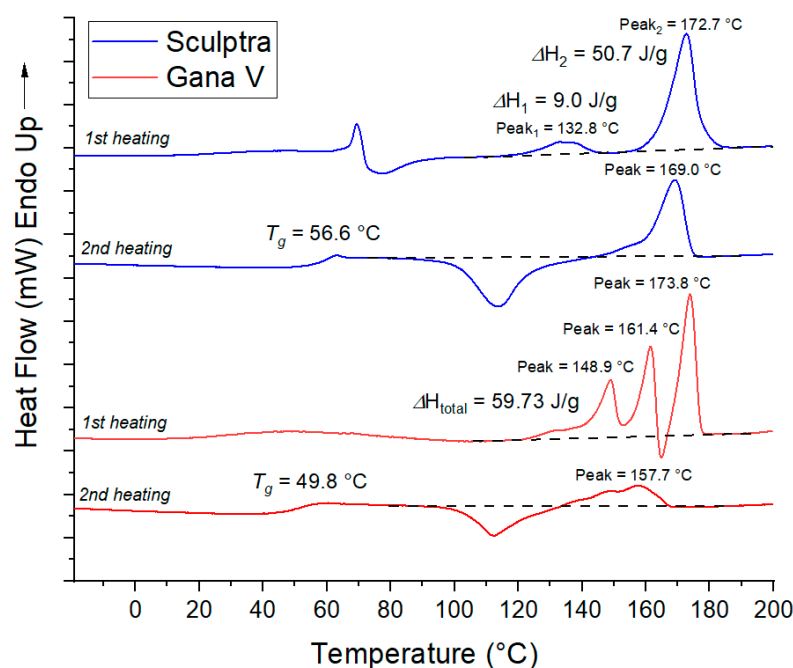


**Figure 2.** DSC curves of microspheres in Sculptra и Gana V fillers.

Molecular weight. Another important parameter is the molecular weight of PLA. In the study [6], the biological effect of fillers based on poly(*L*-lactic acid) with an average molecular weight ranging from 32 to 290 kDa was compared. It was observed that the inflammatory reaction was more prolonged for fillers based on higher-molecular-weight polymers, while the level of inflammation was approximately the same for all samples. Over the observation period of 13 months, the highest collagen production was found for the PLA sample with a number-average molecular weight  $M_n$  (arithmetic average of the molecular masses of the individual macromolecules) of 208 kDa. In this study, the molecular weight characteristics of PLA in the investigated fillers were determined using the gel permeation chromatography method. The obtained results are presented in Table 2.

**Table 2.** Composition and molecular weight characteristics of polylactic acid (PLA) in dermal fillers.

Filler	Composition	$M_w$ , kDa	$M_n$ , kDa	$\bar{D}$
Sculptra	Poly( <i>L</i> -lactic acid)	78	31	2.48
Gana V	Poly( <i>L</i> -lactic acid)	114	47	2.45
AestheFill	Poly( <i>D,L</i> -lactic acid)	80	39	2.03
Repart PLA	Poly( <i>D,L</i> -lactic acid)	107	51	2.08

From Table 2, Gana V and Repart PLA exhibit a higher molecular weight ( $M_w \sim 110$  kDa) compared to the samples of AestheFill and Sculptra ( $M_w \sim 80$  kDa). The dispersity ( $\bar{D}$ ), which characterizes the width of the molecular weight distribution, is lower for the AestheFill and Repart PLA. Overall, this can be considered as an advantage of these preparations since a lower  $\bar{D}$  provides a more controlled polymer degradation profile.

### 3.2. Size and Morphology of PLA Microspheres

The particle size of the filler should be sufficiently large (above 20  $\mu\text{m}$ ) to avoid phagocytosis, yet small enough (below 100  $\mu\text{m}$ ) to easily pass through a needle. The diameter and porosity of microspheres can influence the degradation kinetics of the filler and its biological effects.

AestheFill. Scanning electron microscopy (SEM) was employed to investigate the sizes and morphology of the microspheres. Figure 3 presents SEM micrographs of AestheFill without any prior preparation.

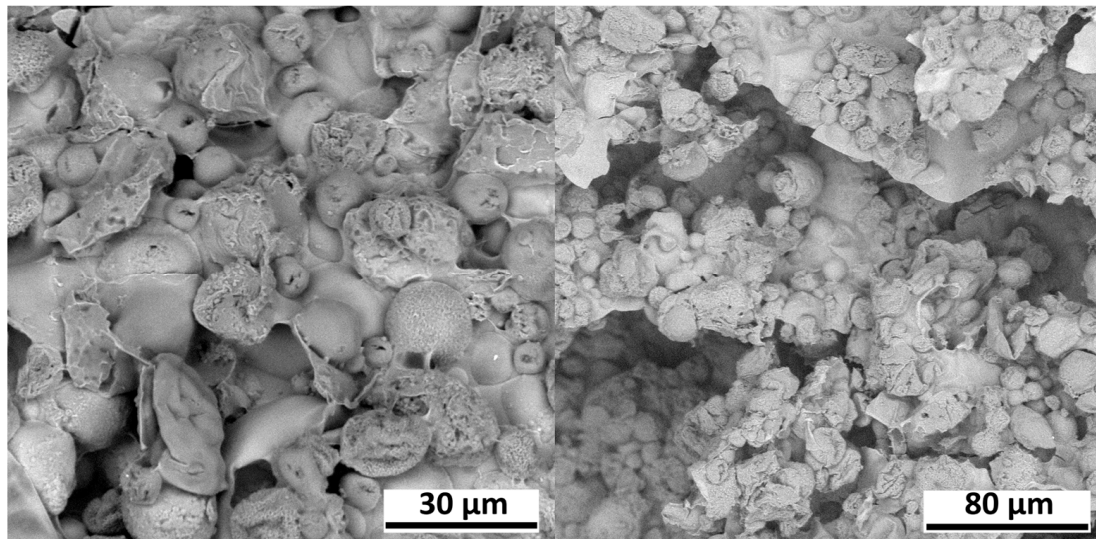


**Figure 3.** Electron microscopy images of AestheFill without any prior preparation.

The images show microspheres with diameters ranging from 10 to 50  $\mu\text{m}$ , immersed in a matrix of Na-carboxymethylcellulose. This matrix complicates the analysis of microspheres, so prior to further investigation, the removal of water-soluble components was performed for all samples. SEM images of the isolated AestheFill microspheres, as well as their size distribution, are presented in Figure 4. The particles exhibit a large surface area, and their shape is close to spherical. The histogram depicting the size distribution of the microspheres demonstrates a single peak, with the average particle size of  $D_{av} = 27 \pm 17 \mu\text{m}$ . The parameter  $D_{90}$  indicates that 90% of all particles have a size of 47  $\mu\text{m}$  or less, while the parameter  $D_{10}$  suggests that 10% of the particles have a size of 8  $\mu\text{m}$  or less.

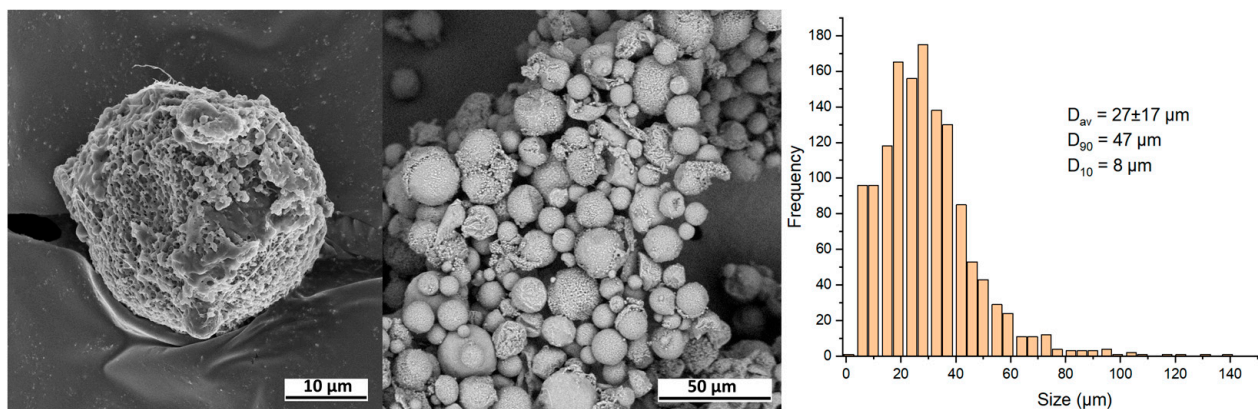


**Figure 4.** SEM images and size distribution of the isolated AestheFill microparticles.

To analyze the internal structure of the microspheres, an individual particle was sliced using a focused ion beam, as shown in Figure 5. Within the cross-section of the particle, irregularly shaped pores with sizes ranging from 2 to 5  $\mu\text{m}$  are visible (pores are indicated by arrows).

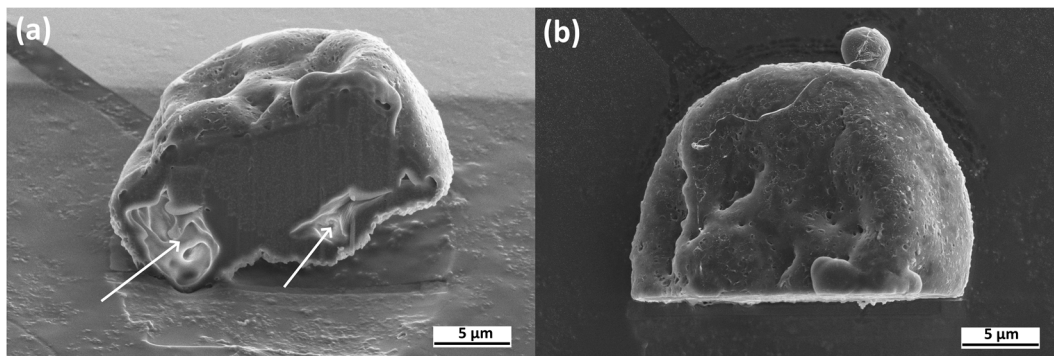


**Figure 5.** SEM images of a cross-section of the individual AestheFill microparticle. Side view (a) and top view (b).

The presence of internal pores in the microspheres is also confirmed by the fact that upon centrifugation, the AestheFill suspension formed a floating fraction on the surface. A smaller fraction of precipitate was also observed, likely consisting of less porous particles. To construct a size distribution histogram, both fractions were analyzed.

Repart PLA. Figure 6 displays SEM images of the Repart PLA sample, revealing that the microspheres exhibit a smooth surface and spherical morphology. The particle diameter ranges from 5 to 80 µm. Based on the analysis of the images, it has been determined that the size distribution of the particles is monomodal, and its size characteristics are similar to those of the AestheFill. The average particle size  $D_{av}$  is  $28 \pm 16$  µm, with  $D_{90} = 50$  µm and  $D_{10} = 10$  µm.

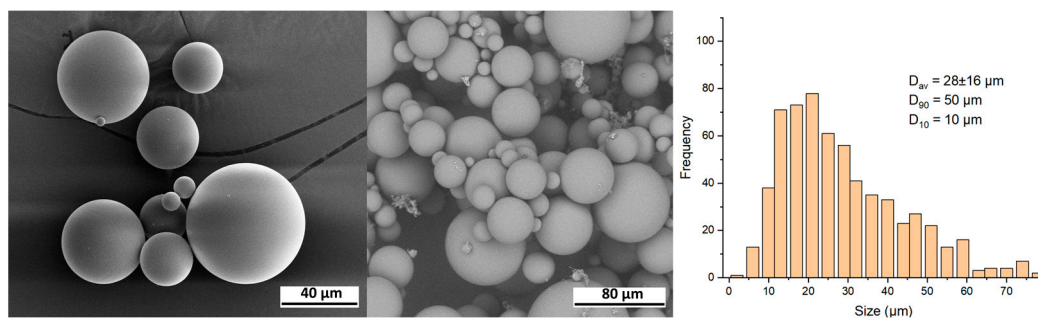


**Figure 6.** SEM images and size distribution of Repart PLA microparticles.

Unlike AestheFill, the Repart PLA microspheres exhibit a smooth surface and do not contain pores. To analyze the internal structure of the Repart PLA microspheres, an individual microsphere was sliced using a focused ion beam, as shown in Figure 7.

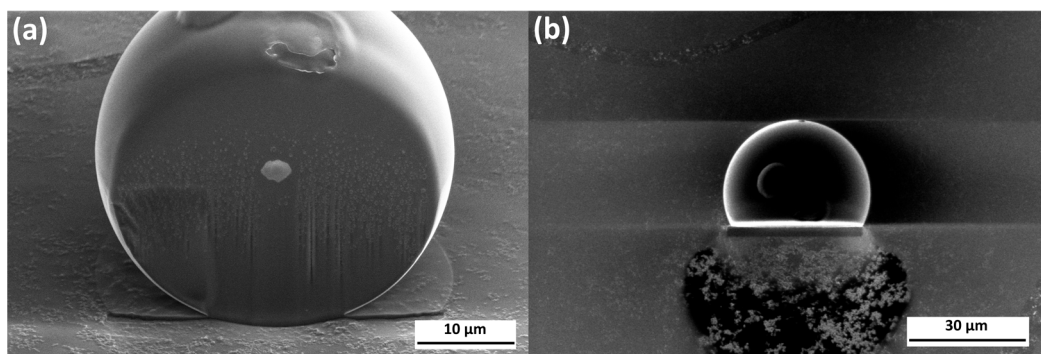


**Figure 7.** SEM images of a cross-section of the individual Repart PLA microparticle. Side view (a) and top view (b).



The images of the cross-section presented in Figure 7 demonstrate the absence of internal pores. The observed defects can be attributed to material degradation caused by the ion beam. The absence of a floating fraction after centrifugation further supports the assumption of a solid (non-porous) internal structure of the microspheres.

Gana V. Upon centrifugation, the Gana V sample separated into a sediment and a floating fraction, similar to the AestheFill. As shown in the SEM images in Figure 8, the particles exhibit an irregular shape and porous morphology. The analysis of the images revealed that the particles in Gana V are larger compared to AestheFill and Repart PLA. The average particle size  $D_{av}$  is  $42 \pm 22 \mu\text{m}$ , and the parameters  $D_{90}$  and  $D_{10}$  are  $58 \mu\text{m}$  and  $18 \mu\text{m}$ , respectively. The size distribution is monomodal.

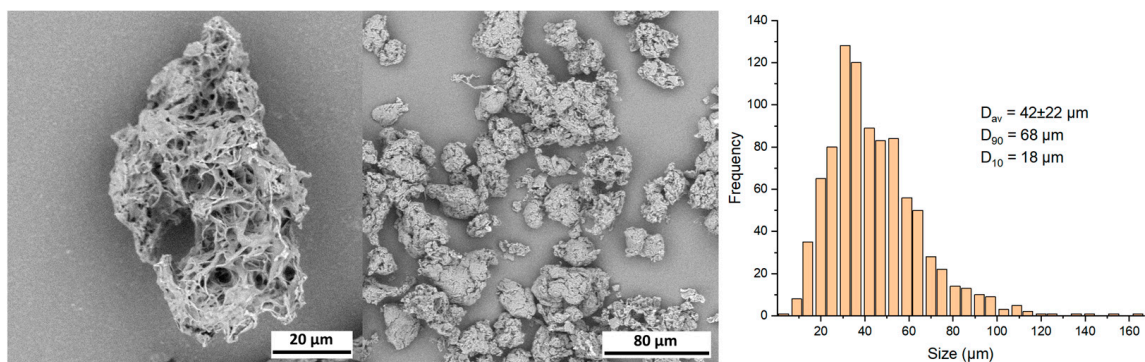


**Figure 8.** SEM images and size distribution of Gana V microparticles.

Sculptra. Figure 9 displays SEM images of the Sculptra sample. The particles exhibit an irregular flat plate-like shape. They do not possess any visible pores, which is also confirmed by the formation of only a sediment fraction after centrifugation.

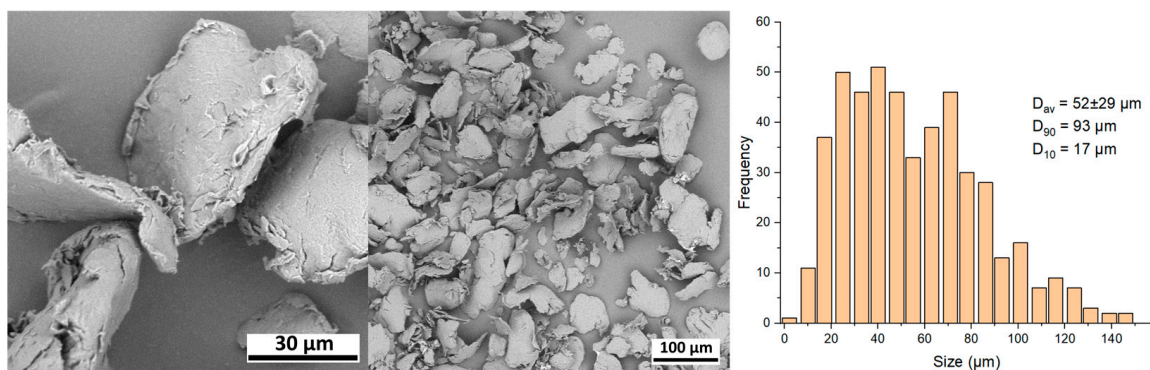


**Figure 9.** SEM images and size distribution of Sculptra microparticles.

The microspheres in Sculptra exhibited the largest size among the investigated fillers. The average particle size  $D_{av}$  is  $52 \pm 29 \mu\text{m}$ , and the parameters  $D_{90}$  and  $D_{10}$  are equal to  $93 \mu\text{m}$  and  $17 \mu\text{m}$ , respectively. The size distribution is relatively broad, with a small fraction of particles having a diameter of  $100 \mu\text{m}$  and above.

To summarize, the PLA microparticles in the studied fillers have different sizes and size distribution, as well as different morphologies, which can be spherical or irregular in shape, and either porous or non-porous. Normally, the more narrow size distribution is preferred, since a fraction of too small (i.e.,  $<20 \mu\text{m}$ ) microparticles can be processed by phagocytes, while a fraction of too large particles (i.e.,  $>100 \mu\text{m}$ ) can become stuck in the needle during injection. Concerning the shape of the particle, the smooth regular morphology might be more favorable, since particles with rough surfaces and irregular shapes can cause a foreign body granuloma as a dominant characteristic of the long-term biological response [13].

### 3.3. Hydrolytic Degradation Studies

The degree and duration of the inflammatory reaction, as well as the stimulation of collagen synthesis, depend on the degradation profile of PLA microspheres in the filler. In the study [6], it was demonstrated that when the degradation of low-molecular-weight poly(lactic-co-glycolic acid) or low-molecular-weight polylactic acid microspheres occurs too rapidly, the inflammation subsides quickly, but the volume of newly synthesized collagen is relatively small. A more pronounced neocollagenesis was observed for medium- and high-molecular-weight PLA microspheres, which also exhibited a longer duration of the inflammatory response. Therefore, the investigation of the degradation of PLA microspheres is an important issue.

Hydrolytic degradation is one of the main mechanisms of polylactic acid breakdown, leading to the cleavage of ester bonds in the polymer chains and a reduction in molecular weight. According to a bulk degradation mechanism, water readily diffuses into the microspheres, causing hydrolysis not only at the surface, but also throughout the particle volume. The molecular weight of PLA decreases until the formed short chains (1 kDa and below) become soluble in water. At the final stage, these oligomers are eliminated from the particle, leading to its gradual dissolution and disappearance.

To study the degradation of microspheres, the samples were suspended in phosphate buffer (distilled water for AestheFill) and incubated for 9 months at 37 °C. Samples were taken at different time points to determine the molecular weight of PLA, which characterizes the degree of degradation. The morphology of the microspheres was also investigated using electron microscopy at the sixth month time point. The research revealed that for all samples, except Gana V, the molecular weight distribution at all time points is monomodal and gradually shifts toward lower molecular weights (Figure 10a,c,d), confirming the bulk degradation mechanism.

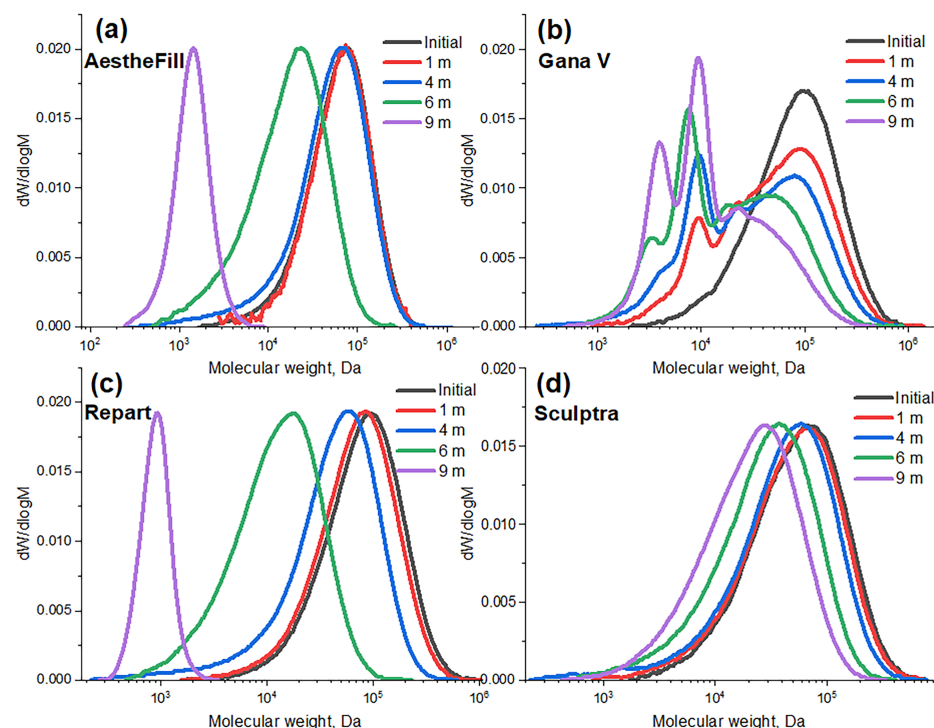


**Figure 10.** Molecular weight distributions of PLA during the hydrolytic degradation of microparticles in different fillers.

Starting from the first month, the molecular weight distribution of PLA in Gana V microspheres shows a second peak in the region of lower molecular weights (~8 kDa) in addition to the main peak (Figure 10b). Furthermore, the molecular weight distribution significantly broadens during the degradation process. Already at the one-month time



point, the dispersity ( $\mathcal{D}$ ) is 3.9, and at the six-month time point, it reaches a value of 4.3. Such a degradation pattern may be associated with the presence of regions that are more susceptible to hydrolysis, such as the surface layers of the particles. These results indicate a heterogeneous degradation accompanied by the formation of low molecular weight oligomers of lactic acid from the early stages. Depending on the concentration of these oligomers in the implantation area, such a degradation profile can be both a positive and a negative factor. On the one hand, the increased concentration of acidic ( $-\text{COOH}$ ) groups at early stages may contribute to maintaining a moderate level of inflammation, leading to an increased collagen production. On the other hand, an excessively high concentration of lactic acid oligomers can cause acidification and an undesirably strong inflammatory reaction. Only in vivo experiments can show how the observed degradation profile specifically influences the biological effect of the Gana V filler.

In Figure 11, the absolute and relative (normalized to the initial) weight-average ( $M_w$ ) molecular weights of polylactic acid at different time points of degradation are presented. Overall, the degradation rate increases in the following order: Sculptra, Gana V, AestheFill, Repart PLA.

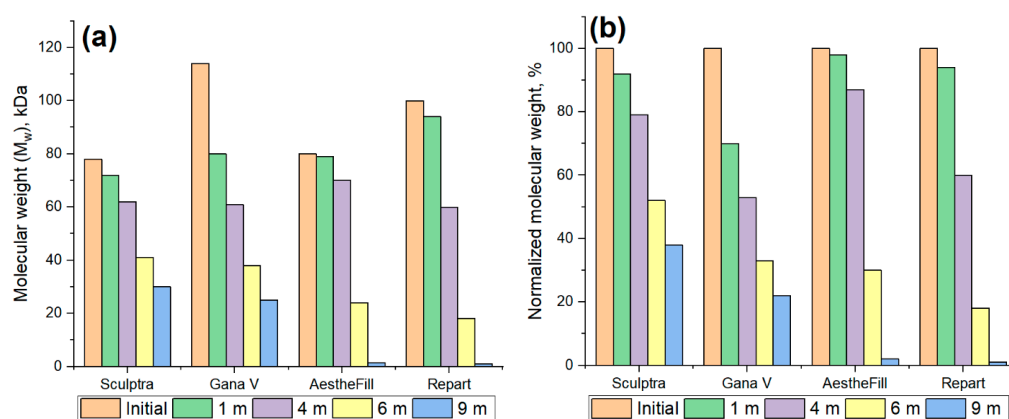


**Figure 11.** Absolute (a) and normalized (b) weight-average molecular weight ( $M_w$ ) of PLA during the hydrolytic degradation of the microparticles over a period of 9 months.

The Repart PLA sample based on poly(*D,L*-lactic acid) demonstrated the most rapid degradation, with the  $M_w$  value decreasing by 5 times (from 100 to 18 kDa) over 6 months. After 9 months, it completely decomposed into low-molecular-weight water-soluble oligomers. For the porous particles of poly(*D,L*-lactic acid) in AestheFill, a delayed degradation effect was observed for up to 4 months, after which the process became much more intensive, and these microspheres almost completely degraded within 9 months. The Sculptra based on poly(*L*-lactic acid) exhibited the slowest degradation rate, with its molecular weight decreasing from 78 to 30 kDa over 9 months. The porous PLA microparticles of Gana V degraded faster than the non-porous Sculptra particles, with the weight-average molecular weight decreasing from 114 to 25 kDa over 9 months.

In general, the observed patterns correspond to the known data that poly(*L*-lactic acid) degrades slower than poly(*D,L*-lactic acid) [4]. It is necessary to consider that degradation kinetics are influenced by parameters such as the degree of polymer crystallinity, particle size [14], and porosity [15]. The presence of interconnected pores can slow down the degradation process due to the absence of an autocatalytic effect caused by the accumulation of acidic degradation products in the material.

The analysis of microparticles after 6 months of degradation using electron microscopy revealed that the Sculptra and Gana V samples based on poly(*L*-lactic acid) maintained their shape and size, while the morphology of AestheFill and Repart PLA fillers changed significantly (Figure 12). After 6 months, the AestheFill microparticles formed a continuous polymeric layer with pores and some spherical particles with a size of less than 5  $\mu\text{m}$  (Figure 12a). The smooth spherical particles of the Repart PLA sample after 6 months of

degradation shrank, and pores were formed on the surface and in bulk. This observation suggests the leaching of degradation products from the particle volume through the pores (Figure 12b,c).

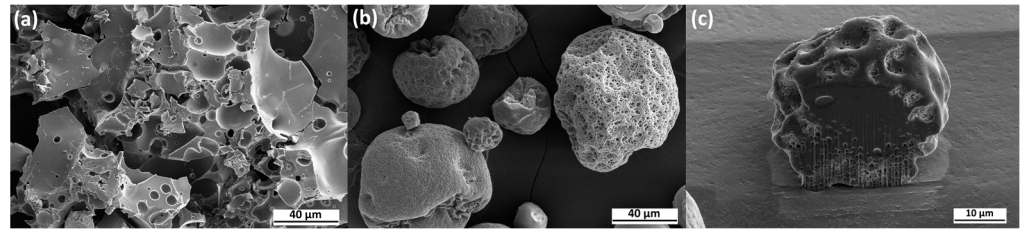


**Figure 12.** SEM images after 6 months of the degradation of microparticles in AestheFill (a), Repart PLA (b). Cross-section of Repart PLA microparticle (c).

The hydrolytic degradation studies of microparticles revealed that, despite all the manufacturers claim an almost similar degradation period of around 2 years, the AestheFill and Repart PLA consisting of poly(*D,L*-lactic acid) demonstrated a much faster hydrolysis, with the period of total hydrolytic degradation estimated as 10–12 months. The process was accompanied by changes in the morphology of microspheres. Poly(*L*-lactic acid)-based fillers Sculptra and Gana V degraded slower with no changes in morphology after 9 months and a decrease in molecular weight to 25–30 kDa. The projected period for a complete resorption of these microparticles can be close to 2 years, as claimed in the manual. It is worth noting that the *in vivo* degradation profile can be affected by the presence of enzymes and other factors.

#### 4. Conclusions

A comprehensive study was conducted on the physicochemical characteristics of polylactic acid microspheres in commercially available fillers from different manufacturers. It was found that in Sculptra and Gana V fillers, the microspheres consist of semi-crystalline poly(*L*-lactic acid) and exhibit different morphologies with average sizes of 52  $\mu\text{m}$  and 42  $\mu\text{m}$ , respectively. The microspheres in Repart PLA and AestheFill consist of amorphous poly(*D,L*-lactic acid) and have the same average diameter of 28  $\mu\text{m}$ . However, Repart PLA microspheres are smooth and spherical with no visible pores, while AestheFill microspheres are spherical, have a large surface area, and exhibit high porosity. The differences in physicochemical characteristics of the microspheres are reflected in the kinetics of hydrolytic degradation at 37 °C. The degradation rate increases in the following order: Sculptra, Gana V, AestheFill, Repart PLA. After 9 months, microspheres based on amorphous poly(*D,L*-lactic acid) in AestheFill and Repart PLA fillers have almost completely degraded, while for Sculptra and Gana V samples based on poly(*L*-lactic acid), the reduction in molecular weight over the same period was 62% and 78%, respectively.

The results of the present research in combination with further biological studies may pave the way for understanding the effect of these characteristics on tissue response and the synthesis of *de novo* collagen, as well as the development of new-generation dermal fillers with improved safety and efficacy.

**Author Contributions:** Conceptualization, N.G.S. and A.A.G.; methodology, N.G.S.; validation, K.T.K.; formal analysis, P.N.A.; investigation, N.G.S., P.N.A. and K.T.K.; data curation, N.G.S.; writing—original draft preparation, N.G.S. and K.T.K.; writing—review and editing, N.G.S. and K.T.K.; visualization, K.T.K.; supervision, N.G.S.; project administration, N.G.S.; funding acquisition, A.A.G. All authors have read and agreed to the published version of the manuscript.

**Funding:** This research was funded by Neroly Ltd. (contract №030822).

**Institutional Review Board Statement:** Not applicable.

**Informed Consent Statement:** Not applicable.

**Data Availability Statement:** The data presented in this study are available on request from the corresponding author.

**Acknowledgments:** Measurements were performed using the equipment of the Center for Collective Use «Polymer Research Center» of ISPM RAS. Authors are grateful to S. Malakhov and P. Dmitryakov for their help with the interpretation of results of SEM and DSC studies.

**Conflicts of Interest:** Neroly Ltd. is an official distributor of the AestheFill filler in the Russian Federation. The funders had no role in the design of the study; in the collection, analyses, or interpretation of data; in the writing of the manuscript, or in the decision to publish the results.

## References

1. Narins, R.S.; Mariwalla, K. 1–9: History of Fillers. In *Dermal Fillers*; S. Karger AG: Basel, Switzerland, 2018; Volume 4.
2. Sánchez-Carpintero, I.; Candelas, D.; Ruiz-Rodríguez, R. Dermal Fillers: Types, Indications, and Complications. *Actas Dermo-Sifiliográficas* **2010**, *101*, 381–393. [[CrossRef](#)] [[PubMed](#)]
3. Ramot, Y.; Haim-Zada, M.; Domb, A.J.; Nyska, A. Biocompatibility and safety of PLA and its copolymers. *Adv. Drug Deliv. Rev.* **2016**, *107*, 153–162. [[CrossRef](#)] [[PubMed](#)]
4. Ginjupalli, K.; Shavi, G.V.; Averineni, R.K.; Bhat, M.; Udupa, N.; Upadhya, P.N. Poly( $\alpha$ -hydroxy acid) based polymers: A review on material and degradation aspects. *Polym. Degrad. Stab.* **2017**, *144*, 520–535. [[CrossRef](#)]
5. Gao, Q.; Duan, L.; Feng, X.; Xu, W. Superiority of poly(L-lactic acid) microspheres as dermal fillers. *Chin. Chem. Lett.* **2021**, *32*, 577–582. [[CrossRef](#)]
6. Zhang, Y.; Liang, H.; Luo, Q.; Chen, J.; Zhao, N.; Gao, W.; Pu, Y.; He, B.; Xie, J. In vivo inducing collagen regeneration of biodegradable polymer microspheres. *Regen. Biomater.* **2021**, *8*, rbab042. [[CrossRef](#)] [[PubMed](#)]
7. Fitzgerald, R.; Bass, L.M.; Goldberg, D.J.; Graivier, M.H.; Lorenc, Z.P. Physicochemical Characteristics of Poly-L-Lactic Acid (PLLA). *Aesthetic Surg. J.* **2018**, *38*, 13–17. [[CrossRef](#)] [[PubMed](#)]
8. Christen, M.O. Collagen Stimulators in Body Applications: A Review Focused on Poly-L-Lactic Acid (PLLA). *Clin. Cosmet. Investig. Dermatol.* **2022**, *15*, 997–1019. [[PubMed](#)]
9. Oh, S.; Lee, J.H.; Kim, H.M.; Batsukh, S.; Sung, M.J.; Lim, T.H.; Lee, M.H.; Son, K.H.; Byun, K. Poly-L-Lactic Acid Fillers Improved Dermal Collagen Synthesis by Modulating M2 Macrophage Polarization in Aged Animal Skin. *Cells* **2023**, *12*, 1320. [[CrossRef](#)] [[PubMed](#)]
10. Lin, C.Y.; Lin, J.Y.; Yang, D.Y.; Lee, S.H.; Kim, J.Y.; Kang, M. Efficacy and safety of poly-D,L-lactic acid microspheres as subdermal fillers in animals. *Plast. Aesthetic Res.* **2019**, *6*, 16.
11. Yang, D.Y.; Ko, K.; Lee, S.H.; Lee, W.K. A Comparison of the Efficacy and Safety Between Hyaluronic Acid and Poly(lactic Acid Filler Injection in Penile Augmentation: A Multicenter, Patient/Evaluator-Blinded, Randomized Trial. *J. Sex. Med.* **2019**, *16*, 577–585.
12. Farah, S.; Anderson, D.G.; Langer, R. Physical and mechanical properties of PLA, and their functions in widespread applications—A comprehensive review. *Adv. Drug Deliv. Rev.* **2016**, *107*, 367–392. [[PubMed](#)]
13. Laeschke, K. Biocompatibility of microparticles into soft tissue fillers. *Semin. Cutan. Med. Surg.* **2004**, *23*, 214–217. [[CrossRef](#)] [[PubMed](#)]
14. Dunne, M.; Corrigan, I.; Ramtoola, Z. Influence of particle size and dissolution conditions on the degradation properties of polylactide-co-glycolide particles. *Biomaterials* **2000**, *21*, 1659–1668. [[CrossRef](#)]
15. Odelius, K.; Höglund, A.; Kumar, S.; Hakkarainen, M.; Ghosh, A.K.; Bhatnagar, N.; Albertsson, A.C. Porosity and Pore Size Regulate the Degradation Product Profile of Polylactide. *Biomacromolecules* **2011**, *12*, 1250–1258. [[CrossRef](#)]

**Disclaimer/Publisher's Note:** The statements, opinions and data contained in all publications are solely those of the individual author(s) and contributor(s) and not of MDPI and/or the editor(s). MDPI and/or the editor(s) disclaim responsibility for any injury to people or property resulting from any ideas, methods, instructions or products referred to in the content.